

Divergence-free multi-mode circuit quantum electrodynamics

Mario F. Gely,^{1,*} Adrian Parra-Rodriguez,^{2,*} Daniel Bothner,¹
Ya. M. Blanter,¹ Sal J. Bosman,¹ Enrique Solano,^{2,3} and Gary A. Steele¹

¹*Kavli Institute of NanoScience, Delft University of Technology,
PO Box 5046, 2600 GA, Delft, The Netherlands*

²*Department of Physical Chemistry, University of the Basque Country UPV/EHU, Apartado 644, 48080 Bilbao, Spain*

³*IKERBASQUE, Basque Foundation for Science, Maria Diaz de Haro 3, 48013 Bilbao, Spain*

(Dated: December 13, 2024)

Circuit quantum electrodynamics studies the interaction of artificial atoms and electromagnetic modes constructed from superconducting circuitry. While the theory of an atom coupled to one mode of a resonator is well studied, considering multiple modes leads to divergences which are not well understood. Here, we introduce a full quantum model of a multi-mode resonator coupled to a Josephson junction atom. Using circuit quantization, we find a Hamiltonian in which parameters of the atom are naturally renormalized as additional modes are considered. In our model, we circumvent the divergence problem, and its formulation reveals a physical understanding of the mechanisms of convergence in ubiquitous models in circuit quantum electrodynamics.

Quantum electrodynamics (QED) explores one of the most fundamental interactions in nature, that of light and matter. In a typical cavity QED scenario, an individual atom interacts through its dipole moment with the electric field of cavity modes, as depicted in Fig. 1(a). One consequence of this interaction is the Lamb shift of the atomic transition frequencies [1, 2]. Early attempts at calculating this shift led to the first shortcomings of QED theory, mainly that the transition energies of the atom diverge as the infinite electromagnetic modes are considered. Efforts to address these issues gave birth to renormalization theory [3]. Akin to cavity QED is the field of circuit QED [4], where artificial atoms such as anharmonic superconducting LC circuits couple to the modes of a waveguide resonator or an open transmission line. Such systems allow the study of a wealth of quantum effects [5, 6], and are one of the most promising platforms for the realization of quantum processors [7–9]. Despite experimental successes, multi-mode quantum Rabi models in circuit QED suffered from divergences when considering the limit of infinite modes in a waveguide resonator [10, 11]. Aware of this problem, Nigg *et al.* [12] developed the method of black-box quantization to obtain effective Hamiltonians with higher predictive power [13].

In this Letter, we derive a first-principle Hamiltonian model addressing the divergence issues, expressed in the basis of the uncoupled resonator modes and the atom. We consider the case of an artificial atom (AA) formed from an anharmonic LC oscillator [14], capacitively coupled to a quarter-wave ($\lambda/4$) transmission line resonator [15] as depicted in Fig. 1(b), with a focus on addressing the divergences of the atomic Lamb shift. The AA is a superconducting island connected to ground through a Josephson junction characterized by its Josephson energy E_J . It has a capacitance to ground C_J and is coupled to the voltage anti-node of the resonator, with characteristic impedance Z_0

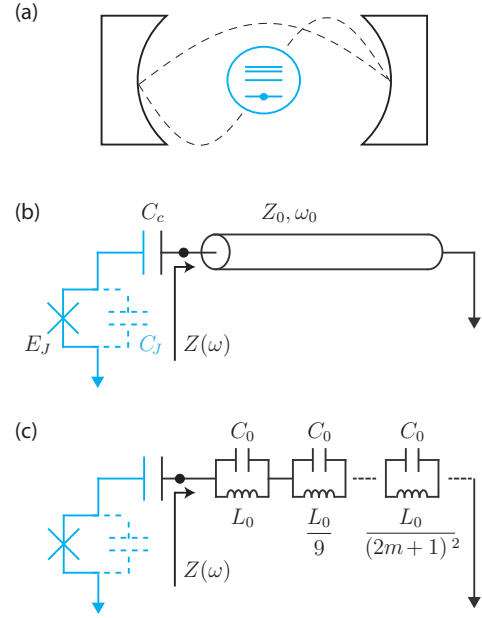


FIG. 1. (a) Schematic representation of cavity QED: A multi-level atom (in blue) coupled to the electromagnetic cavity modes (dashed black lines). (b) Circuit QED example covered in this work: A Josephson junction anharmonic LC oscillator, or “artificial atom”, coupled to modes of a transmission line. (c) Lumped element equivalent of (b).

and fundamental mode frequency $\omega_0/2\pi$, through a capacitance C_c [16]. The Josephson junction acts as a non-linear inductor, providing a source of single-photon anharmonicity in the oscillations of current flowing through it. In order to clearly illustrate the most novel aspect of our model, the renormalization of the charging energy, we first consider the case $C_J = 0$. The case of $C_J > 0$ is discussed at the end of this article and in detail in the Supplementary Material [17].

Circuit Hamiltonian — We consider a Hamiltonian in which each uncoupled harmonic mode of the resonator, with resonance frequency ω_m and annihilation operator \hat{a}_m , is coupled to the transition between the bare atomic states $|i\rangle, |j\rangle$ with energies $\hbar\epsilon_i, \hbar\epsilon_j$ through a coupling strength $\hbar g_{m,i,j}$ [18, 19]. We derive such a Hamiltonian by constructing a lumped element equivalent circuit, or Foster decomposition, of the transmission line resonator as represented in Fig. 1(c). The input impedance of a shorted transmission line, at a distance $\lambda/4$ from the short, $Z(\omega) = iZ_0 \tan(\pi\omega/(2\omega_0))$, is equal to that of an infinite number of parallel LC resonators with capacitances $C_0 = \pi/(4\omega_0 Z_0)$ and inductances $L_m = 4Z_0/((2m+1)^2\pi\omega_0)$. In order to consider a finite number of modes M in the model, one replaces the $m \geq M$ LC circuits in Fig. 1(c) by a short circuit to ground. This removes the $m \geq M$ resonances in the resonator input impedance $Z(\omega)$ with little effect on $Z(\omega)$ for $\omega \ll \omega_M$. The focus of this Letter is on the evolution of the Hamiltonian parameters as a function of this system size M , and the consequences on the energy spectrum. Using the tools of circuit quantization [20], we obtain as Hamiltonian of the system [17]

$$\begin{aligned} \hat{H}^{(M)} = & \sum_i \hbar\epsilon_i^{(M)} |i\rangle^{(M)} \langle i|^{(M)} + \sum_{m=0}^{m < M} \hbar\omega_m \hat{a}_m^\dagger \hat{a}_m \\ & + \sum_{i,j} \sum_{m=0}^{m < M} \hbar g_{m,i,j}^{(M)} |i\rangle^{(M)} \langle j|^{(M)} (\hat{a}_m + \hat{a}_m^\dagger). \end{aligned} \quad (1)$$

The eigenfrequencies of the resonators higher modes ω_m are related to that of the fundamental mode through $\omega_m = (2m+1)\omega_0$. The coupling strength $\hbar g_{m,i,j}^{(M)} = 2eV_{\text{zpf},m} \langle i|^{(M)} \hat{N}_J |j\rangle^{(M)}$ scales with the square root of the mode number m through the zero-point voltage fluctuations of the m -th mode $V_{\text{zpf},m} = \sqrt{2m+1} \sqrt{\hbar\omega_0/2C_0}$. Since we will concentrate on the frequency and coupling of the first atomic transition $|g\rangle \rightarrow |e\rangle$, we use the shorthand $\omega_a^{(M)} = \epsilon_e - \epsilon_g$ and $g_m^{(M)} = g_{m,g,e}^{(M)}$ throughout this Letter.

The (bare) AA eigenstates $|i\rangle^{(M)}$ and energies $\hbar\epsilon_i^{(M)}$ in Eq. (1) are those that diagonalize the Hamiltonian

$$\hat{H}_{\text{AA}}^{(M)} = 4E_C^{(M)} \hat{N}_J - E_J \cos(\hat{\delta}). \quad (2)$$

Here \hat{N}_J is the quantum number of Cooper-pairs on the island conjugate to $\hat{\delta}$ the superconducting phase difference across the junction, and $E_C^{(M)}$ is the charging energy of the island. This choice of the decomposition of the Hamiltonian is one in which the bare atom corresponds to purely anharmonic degrees of freedom (currents flowing only through the junction) and the bare cavity to purely harmonic degrees of freedom (currents flowing only through the linear cavity inductors).

The crucial consequence of quantizing our model is a renormalization of the parameters of the Hamiltonian

as modes are added. In particular, the charging energy $E_C^{(M)}$ of the (bare) AA depends explicitly on the number of modes included in the equivalent circuit:

$$E_C^{(M)} = \frac{e^2 C_0 + MC_c}{2 C_0 C_c}. \quad (3)$$

For the case of $M \rightarrow \infty$ with $C_J = 0$, the charging energy of the bare atom diverges. This divergence arises from the definition of the bare atom as current oscillations flowing only through the junction. As $M \rightarrow \infty$, the impedance path through only the series capacitors of the resonator equivalent circuit diverges. Charge from currents through the junction can no longer oscillate on C_c and $\omega_a^{(M)}$ diverges. For the case of $M = 1$ and $C_c \ll C_0$, Eq. (3) simplifies to the standard definition of the charging energy $E_C = e^2/2C_c$ [14]. With $M > 1$, we will see that a more complex picture emerges.

Renormalization of the atomic parameters — In Fig. 2, we explore the renormalization of the parameters of our model as the number of modes M is increased. Through equation 2, both the eigenstates $|i\rangle^{(M)}$ and coupling strengths $g_m^{(M)}$ also depend on M . For a fixed number of modes M , the coupling $g_m^{(M)}$ of the atom to mode m scales with the square root of the mode number m : $g_m^{(M)} = g_0^{(M)} \sqrt{2m+1}$. From this coupling, each mode will induce a Lamb shift of the atomic energy $\chi_m/\hbar \simeq -2(g_m^{(M)})^2/\omega_m = -2(g_0^{(M)})^2/\omega_0$, a formula valid when ω_m is much larger than the bare atomic frequency. With the typical assumption of coupling and bare atomic frequency independent of M , summing the Lamb shifts of every mode would lead to diverging values of the dressed atomic frequencies. This leads to the divergences found in typical multi-mode extensions of the quantum Rabi model.

In the model presented here, however, we find that the full quantization of the lumped-element circuit leads to a Hamiltonian in which both the bare atomic frequency ω_a and the couplings to the modes g_m are explicitly dependent on the number of modes M included in the model. As the number of modes M in the model increases, the bare atomic couplings $g_m^{(M)}$, (a) and (b), are suppressed, and the bare atomic frequency $\omega_a^{(M)}$, (c), increases, diverging for an infinite number of modes. As we will see, however, this divergence is removed in the dressed transition energy of the atom when including the Lamb-shift from higher modes of the resonator.

As an illustration of how renormalization in our model leads to convergence of the spectrum, let us consider the case shown in Fig.2 (d) - (e) in which the fundamental mode is resonant with the atomic frequency $\omega_a^{(1)}$ when $M = 1$ (Fig. 2(d)). Including an additional mode with frequency ω_1 will lead to an upwards shift of the bare atomic transition $\omega_a^{(1)} \rightarrow \omega_a^{(2)} > \omega_a^{(1)}$ and a change of the coupling $g_0^{(1)} \rightarrow g_0^{(2)} < g_0^{(1)}$ through the

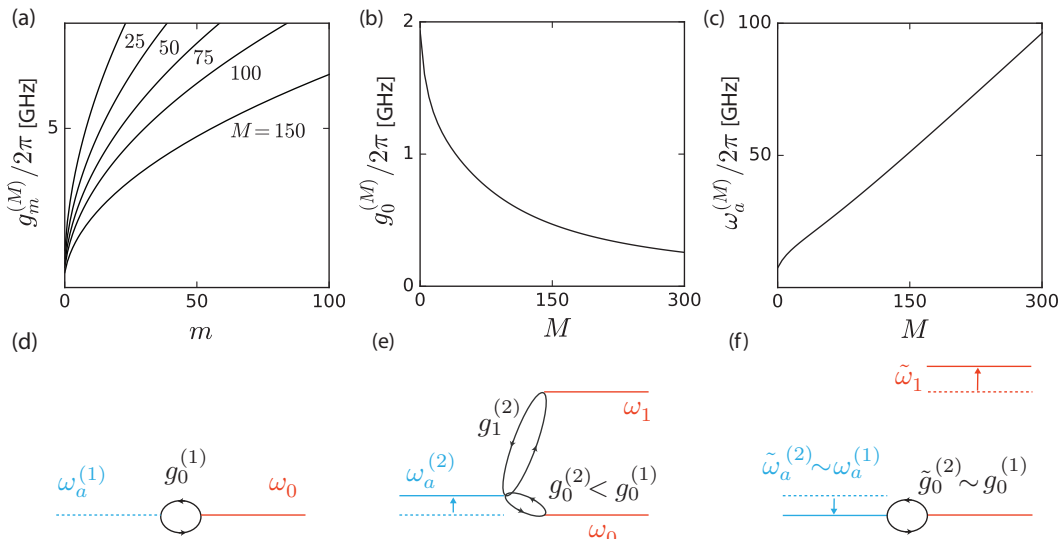


FIG. 2. Renormalization of the Hamiltonian parameters and dressing of the atom by higher modes. For the plots, we choose $\omega_0/2\pi = 10$ GHz, $Z_0 = 50 \Omega$, $C_c = 50$ fF and $E_J/h = 20$ GHz. Although this places the AA in the Transmon limit, we note that the scaling shown in the figure are exact for all regimes, including the CPB limit. (a) Coupling of the ground to first excited state transition of the atom $|g\rangle \rightarrow |e\rangle$ to the resonator modes as a function of the mode number m : $\hbar g_m^{(M)} = \sqrt{2m+1} V_{zpf,0} 2e \langle g | e \rangle^{(M)} \hat{N}_J |e\rangle^{(M)}$. The M -dependence of the coupling is detailed in (b). (b),(c) Renormalization of the coupling strength and the atomic frequency through the change in charging energy $E_C^{(M)}$ as a function of M . For large M , the coupling diminishes with $1/M$ and the atomic frequency increases linearly with M . (d-f) Schematic energy diagrams of the renormalization procedure in the case of the atom and fundamental mode at resonance. (a) $M = 1$ (b) $M = 2$. Adding a mode shifts the bare atomic energy upwards and changes the values of the couplings. (f) Dressing the atom with the second mode results in a dressed atomic state with atomic frequency and coupling to the $m = 1$ mode close to that of the $M = 1$ model.

renormalization of the charging energy (Fig. 2(e)). Diagonalizing the subsystem of the atom and mode 1 in our model, the transition energy of the atom is shifted down again near resonance with the fundamental mode $\omega_a^{(2)} \rightarrow \tilde{\omega}_a^{(2)} \sim \omega_a^{(1)}$ by the dispersive shift, and the coupling of the atomic transition to the fundamental mode is increased $g_0^{(2)} \rightarrow \tilde{g}_0^{(2)} \sim g_0^{(1)}$ (Fig. 2(f)). In this way, the resulting vacuum Rabi splitting of the fundamental mode is found to be similar to that of the $M = 1$ model, despite the decrease in the bare coupling rates $g_0^{(2)}$.

Note that in our model, the value of $E_J/E_C^{(M)}$ of the bare atom, which determines its anharmonicity [14], is also a function of M . It would seem that in the limit $M \rightarrow \infty$, the bare atom would be deep in the Cooper pair box limit. However, including the hybridization with the cavity, the low energy sector of $H^{(M+1)}$ is well approximated by a model with M modes where the charging energy is not $E_C^{(M)}$ but

$$\tilde{E}_C^{(M)} = E_C^{(M+1)} - \hbar(\bar{g}_M^{(M+1)})^2/4\omega_M, \quad (4)$$

where $\bar{g}_m^{(M)}$ is the coupling constant without the dipole moment $\langle i | e \rangle^M \hat{N}_J |j\rangle^M$. For this to hold, $\hbar\omega_M$ must be larger than the characteristic energy of the low energy sector of $H^{(M)}$. In this case, the vacuum of the $(M+1)$ -th mode, shifted by $(\bar{g}_M^{(M+1)}/\omega_M) \hat{N}_J$, is a good variational

choice for the low lying energy sector of $H^{(M+1)}$. In this subspace, the effective Hamiltonian is of the same form as $H^{(M)}$, but with charging energy $\tilde{E}_C^{(M)}$ [17]. This result matches with the zero-th order of a Schrieffer-Wolff approximation [21, 22]. We can iterate this procedure to a mode L . For $M \rightarrow \infty$, an effective Hamiltonian with L modes will have a finite charging energy

$$\tilde{E}_C^{(L)} = \lim_{M \rightarrow \infty} E_C^{(M)} - \sum_{m \geq L}^M \hbar(\bar{g}_m^{(M)})^2/4\omega_m. \quad (5)$$

The interaction with higher modes therefore modifies the charging energy of the dressed atom, leading to a convergence of the atomic anharmonicity as well. This formula applies for all values of C_J , but for $C_J = 0$, we have $\tilde{E}_C^{(M)} = E_C^{(M)}$, *i.e.*, the dressing from higher modes exactly compensates the renormalization of the charging energy.

In order to illustrate the effectiveness of this renormalization, in Fig. 3 we compare a diagonalization of Hamiltonian (1) to a non-renormalized multi-mode extension of the quantum Rabi model, implemented by removing the M -dependence of the charging energy $E_C^{(M)} \rightarrow e^2/(2C_c)$. The dashed line indicates the result of the Black-box quantization (BB) method [12] as a point of reference. The calculations are performed using the same phys-

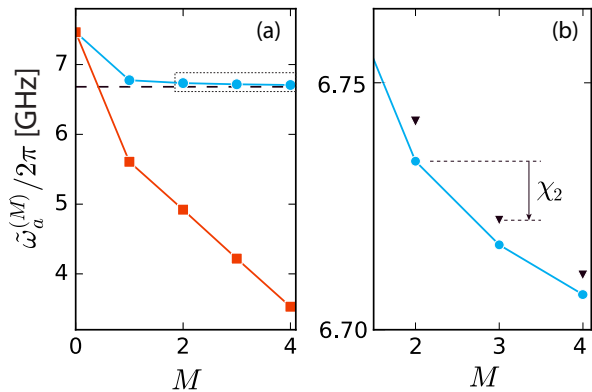


FIG. 3. Calculated spectrum as a function of the number of modes M included in the model. (a) Dots (squares) correspond to a diagonalization of the circuit (non-)renormalized extended-Rabi model. The frequency obtained by Black-box quantization of the circuit Fig. 1(b) (dashed line) provides a point of reference corresponding to the case when all modes are included. (b) Zoom of dashed box in (a). Triangles show the prediction based on a first order classical approximation of the Lamb shift: $\chi_M = \tilde{\omega}_a^{(M+1)} - \tilde{\omega}_a^{(M)} \simeq -2((g_M^{(0)})^2/\omega_M)((\omega_a^{(0)})^2/\omega_M^2)$ [17].

ical parameters as in Fig. 2. Compared to the non-renormalized model, which diverges linearly, a diagonalization of the first-principle Hamiltonian (1) converges towards the value expected from BB.

It is also interesting to note that the corrections from our model are non-perturbative: perturbation theory fails to give a value for the Lamb shift resulting from including an extra mode. Using a circuit analysis of coupled LC oscillators (see [17]), in the Transmon regime, $E_J \gg E_C^{(M)}$, we find an estimate of the shift in the dressed AA energy when including an additional mode in the model given by $\chi_m/\hbar \simeq -2(g_m^2/\omega_m)(\tilde{\omega}_a^2/\omega_m^2)$. This formula can be used to estimate the number of relevant modes to include in a simulation, and can be thought of as a replacement of the usual expression for the Lamb shift $\chi_m^{Lamb}/\hbar \simeq -2g_m^2/\omega_m$.

High-frequency cutoff — In a realistic system, higher modes will tend to decouple from the atom due to several coexisting physical mechanisms [11]. One such mechanism is the capacitance of the Josephson junction C_J . In particular, the capacitive loading of the cavity from the AA illustrated in the inset of Fig. 4 leads to a decreasing impedance to ground $Z_c(\omega) \simeq i(C_J + C_c)/\omega C_J C_c$ at the end of the resonator when $\omega \gg \omega_a$. When the mode frequencies become such that this impedance is lower than the characteristic impedance of the resonator $|Z_c(\omega)| \ll |Z_0|$, this voltage anti-node of the resonator, to which the AA couples, becomes a voltage node, and the coupling vanishes. Additionally, the eigenfrequencies will span from those of a $\lambda/4$ resonator for the lower modes to those of a $\lambda/2$ resonator $\omega_m \rightarrow 2m\omega_0$ for the higher

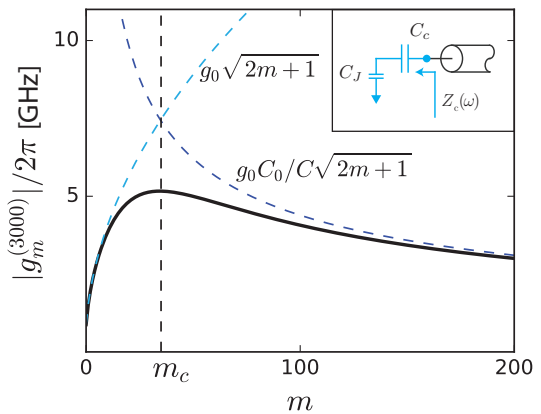


FIG. 4. High-frequency cutoff for $C_J \neq 0$. The capacitive loading at the left boundary of the resonator shown in the inset transforms this point from a voltage anti-node to a voltage node for higher modes. The mode $m_c \simeq 35$ marks this transition. The solid line corresponds to the coupling strength as a function of the number of modes. With $C_J \neq 0$ the coupling strength converges to a non-zero value for large M hence the choice $M = 3000$. Dashed lines: asymptotic values of the coupling, with $g_0 = g_0^{M=3000}$ and $C = C_c C_J / (C_c + C_J)$.

lying modes.

This effect can be captured with the same quantization procedure applied to the circuit in Fig. 1(c) with $C_J \neq 0$ and is detailed in the supplementary material [17]. Mathematically, the cutoff in the coupling is due to a mode-mode coupling term of the form $\sum_{m=0}^{m < M} \sum_{m'=m+1}^{m < M} G_{m,m'}^{(M)} (\hat{a}_m + \hat{a}_m^\dagger)(a_{m'} + a_{m'}^\dagger)$, which arises naturally from the circuit quantization. This is the equivalent of the A^2 term discussed in Refs. [23, 24]. Diagonalizing the Hamiltonian of coupled resonator modes leads to decreasing zero-point voltage fluctuations of the modes at the coupling node. As shown in Fig. 4, with a capacitance to ground $C_J = 5$ fF close to the experimental parameters of Ref. [16], the expected cutoff occurs when $|Z_c(\omega_{m_c})| \simeq |Z_0|$, or equivalently at the mode number $m_c \simeq (C_J + C_c)/2\omega_0 Z_0 C_J C_c$. This mechanism is accompanied by the appearance of an upper bound in the renormalized charging energy, such that Eq. (3) becomes

$$E_C^{(M)} = \frac{e^2}{2} \frac{C_0 + M C_c}{M C_c C_J + C_0 (C_c + C_J)}, \quad (6)$$

and $E_C^{(M)} \rightarrow e^2/2C_J$ for $M \rightarrow \infty$. We emphasize however, that this cutoff is not a necessary condition for the convergence of the energy spectrum: the model described above with $C_J = 0$ converges even in the absence of such a cutoff. This is to be contrasted with typical models of atoms coupled to cavity modes where high frequency cutoffs must be imposed to obtain finite predictions [25].

Conclusion — We have derived a first-principle model of multi-mode circuit quantum electrodynamics which results in convergence of quantities such as the Lamb shift.

Our approach leads to a renormalization of the atomic charging energy which compensates the dispersive energy shift of the higher frequency modes and results in a converging energy spectrum. The formulation of this problem in the context of circuits hints an intuitive picture on how this renormalization arises physically, and it suggests the study of how the proposed physical picture could be applied to other problems in quantum field theory.

Acknowledgments A. P-R and E. S. thank Enrique Rico and Íñigo Egusquiza for useful discussions. M. G. and G. S. thank Yuli V. Nazarov for useful discussions. The authors acknowledge funding from UPV/EHU UFI 11/55, Spanish MINECO/FEDER FIS2015-69983-P, Basque Government IT986-16 and PhD grant PRE-2016-1-0284, the Netherlands Organization for Scientific Research (NWO), the Dutch Foundation for Fundamental Research on Matter (FOM), and the European Research Council (ERC).

* These authors contributed equally to this manuscript.

- [1] W. E. Lamb and R. C. Retherford, *Phys. Rev. Lett.* **72**, 241 (1947).
- [2] D. J. Heinzen, *Phys. Rev. Lett.* **59**, 195 (1988).
- [3] H. A. Bethe, *Phys. Rev. Lett.* **72**, 339 (1947).
- [4] A. Wallraff, D. Schuster, A. Blais, L. Frunzio, R. Huang, J. Majer, S. Kumar, S. Girvin, and R. J. Schoelkopf, *Nature* **431**, 162 (2004).
- [5] D. I. Schuster, A. A. Houck, J. A. Schreier, A. Wallraff, J. M. Gambetta, A. Blais, L. Frunzio, J. Majer, B. Johnson, M. H. Devoret, S. M. Girvin, and R. J. Schoelkopf, *Nature (London)* **445**, 515 (2007).
- [6] L. S. Bishop, J. M. Chow, J. Koch, A. A. Houck, M. H. Devoret, E. Thuneberg, S. M. Girvin, and R. J. Schoelkopf, *Nature Phys.* **5**, 105 (2009).
- [7] M. Takita, A. D. Corcoles, E. Magesan, B. Abdo, M. Brink, A. Cross, J. M. Chow, and J. M. Gambetta, *Phys. Rev. Lett.* **117**, 1 (2016).
- [8] J. Kelly, R. Barends, A. G. Fowler, A. Megrant, E. Jeffrey, T. C. White, D. Sank, J. Y. Mutus, B. Campbell, Y. Chen, Z. Chen, B. Chiaro, A. Dunsworth, I.-C. Hoi, C. Neill, P. J. J. O'Malley, C. Quintana, P. Roushan, A. Vainsencher, J. Wenner, A. N. Cleland, and J. M. Martinis, *Nature (London)* **519**, 66 (2015).
- [9] D. Ristè, S. Poletto, M.-Z. Huang, A. Bruno, V. Vesterinen, O.-P. Saira, and L. DiCarlo, *Nat. Commun.* **6**, 6983 (2015).
- [10] A. A. Houck, J. A. Schreier, B. R. Johnson, J. M. Chow, J. Koch, J. M. Gambetta, D. I. Schuster, L. Frunzio, M. H. Devoret, S. M. Girvin, and R. J. Schoelkopf, *Phys. Rev. Lett.* **101**, 080502 (2008).
- [11] S. Filipp, M. Göppl, J. M. Fink, M. Baur, R. Bianchetti, L. Steffen, and A. Wallraff, *Phys. Rev. A* **83**, 1 (2011).
- [12] S. E. Nigg, H. Paik, B. Vlastakis, G. Kirchmair, S. Shankar, L. Frunzio, M. H. Devoret, R. J. Schoelkopf, and S. M. Girvin, *Phys. Rev. Lett.* **108**, 1 (2012).
- [13] S. M. Girvin, in *Circuit QED: Superconducting Qubits Coupled to Microwave Photons, Proceedings of the Les Houches Summer School* (Vol. 96, Oxford University Press, New York, NY, 2014).
- [14] J. Koch, T. M. Yu, J. Gambetta, A. A. Houck, D. I. Schuster, J. Majer, A. Blais, M. H. Devoret, S. M. Girvin, and R. J. Schoelkopf, *Phys. Rev. A* **76**, 1 (2007).
- [15] D. M. Pozar, *Microwave Engineering* (John Wiley & Sons, New York, 2009).
- [16] S. J. Bosman *et al.* (in preparation).
- [17] See appended supplementary material.
- [18] G. Zhu, D. G. Ferguson, V. E. Manucharyan, and J. Koch, *Phys. Rev. B* **87**, 1 (2013).
- [19] N. M. Sundaresan, Y. Liu, D. Sadri, L. J. Szocs, D. L. Underwood, M. Malekakhlagh, H. E. Tureci, and A. A. Houck, *Phys. Rev. X* **5**, 021035 (2015).
- [20] M. H. Devoret, in *Quantum Fluctuations in Electrical Circuits (Les Houches Session LXIII)*, edited by S. Reynaud, E. Giacobino, and J. Zinn-Justin (Elsevier, New York, 1997).
- [21] J. R. Schrieffer and P. A. Wolff, *Phys. Rev. Lett.* **149**, 491 (1966).
- [22] S. Bravyi, D. P. DiVincenzo, and D. Loss, *Ann. Phys. (New York)* **326**, 2793 (2011).
- [23] S. De Liberato, *Phys. Rev. Lett.* **112**, 1 (2014).
- [24] J. J. García-Ripoll, B. Peropadre, and S. De Liberato, *Sci. Rep.* **5**, 16055 (2015).
- [25] L. Mandel and E. Wolf, *Optical Coherence and Quantum Optics* (Cambridge University Press, Cambridge, 1995).

Supplementary Material: Divergence-free multi-mode circuit quantum electrodynamics

Mario F. Gely,^{1,*} Adrian Parra-Rodriguez,^{2,*} Daniel Bothner,¹
Ya. M. Blanter,¹ Sal J. Bosman,¹ Enrique Solano,^{2,3} and Gary A. Steele¹

¹*Kavli Institute of NanoScience, Delft University of Technology,
PO Box 5046, 2600 GA, Delft, The Netherlands*

²*Department of Physical Chemistry, University of the Basque Country UPV/EHU, Apartado 644, 48080 Bilbao, Spain*

³*IKERBASQUE, Basque Foundation for Science, Maria Diaz de Haro 3, 48013 Bilbao, Spain*

(Dated: December 13, 2024)

S1. DERIVATION OF THE CIRCUIT HAMILTONIAN

The input impedance of a shorted transmission line, at a distance $\lambda_0/4$ from the short (see Ref. [S1]) is given by

$$Z(\omega) = iZ_0 \tan\left(\frac{\pi \omega}{2 \omega_0}\right), \quad (\text{S1})$$

where Z_0 is the characteristic impedance of the waveguide, $\omega_0/2\pi$ is the resonance frequency and λ_0 the wavelength of the fundamental mode of the quarter wave resonator when the AA is replaced by an open termination. The partial fraction expansion of the tangent

$$\tan(z) = \sum_{m=0}^{\infty} \frac{-2z}{z^2 - (m + \frac{1}{2})^2 \pi^2} \quad (\text{S2})$$

leads to an expression for the resonators input impedance which is equal to that of an infinite number of parallel LC resonators. Each of them corresponds to a resonance mode

$$Z(\omega) = iZ_0 \tan\left(\frac{\pi \omega}{2 \omega_0}\right) = \sum_{m=0}^{\infty} \frac{1}{iC_0\omega + \frac{1}{iL_m\omega}}, \quad (\text{S3})$$

$$C_0 = \frac{\pi}{4\omega_0 Z_0}, \quad (\text{S4})$$

$$L_m = \frac{1}{2m+1} \frac{4Z_0}{\pi\omega_0}. \quad (\text{S5})$$

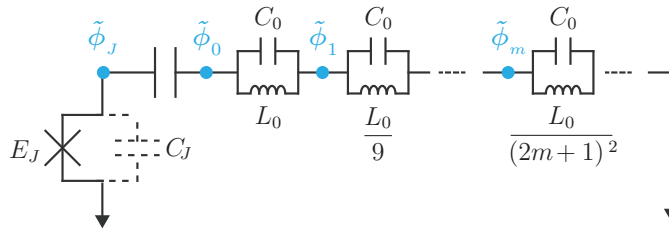


FIG. S1. Circuit quantized in this section. In accordance with Ref. [S2], the degrees of freedom of the circuit are chosen to be the fluxes (indicated in blue) at the nodes of the circuit.

* These authors contributed equally to this manuscript.

We truncate the system to the first M resonators and use the tools of circuit quantization to obtain the corresponding Hamiltonian. Following the methodology given in Refs. [S2] and [S3], we start by defining a set of nodes of the circuit and their corresponding fluxes. We define the flux $\tilde{\phi}$ from the voltage v of that node to ground as

$$\tilde{\phi}(t) = \int_{-\infty}^t v(t') dt'. \quad (\text{S6})$$

As described in Fig. S1, the node corresponding to the superconducting island of the AA is denoted by the subscript J , and we number from 0 to $M-1$ the nodes corresponding to the fluxes from the m -th LC oscillator to the coupling capacitor. The Lagrangian of the system is given by

$$\begin{aligned} \mathcal{L} = & C_J \frac{\dot{\tilde{\phi}}_J^2}{2} + C_c \frac{(\dot{\tilde{\phi}}_J - \dot{\tilde{\phi}}_0)^2}{2} + \sum_{m=0}^{m < M-1} C_0 \frac{(\dot{\tilde{\phi}}_m - \dot{\tilde{\phi}}_{m+1})^2}{2} + C_0 \frac{(\dot{\tilde{\phi}}_{M-1})^2}{2} \\ & + E_J \cos\left(2\pi \frac{\tilde{\phi}_J}{\Phi_0}\right) - \sum_{m=0}^{m < M-1} (2m+1)^2 \frac{(\tilde{\phi}_m - \tilde{\phi}_{m+1})^2}{2L_0} - (2M-1)^2 \frac{(\tilde{\phi}_{M-1})^2}{2L_0}, \end{aligned} \quad (\text{S7})$$

where $\Phi_0 = h/2e$ corresponds to the flux quantum and is not to be confused with $\tilde{\phi}_0$. We now make the change of variables $\phi_m = \tilde{\phi}_m - \tilde{\phi}_{m+1}$ for $0 \leq m < M-1$, leaving the remaining two variables unchanged $\phi_{M-1} = \tilde{\phi}_{M-1}$ and $\phi_J = \tilde{\phi}_J$. The Lagrangian then reads

$$\begin{aligned} \mathcal{L} = & C_J \frac{\dot{\phi}_J^2}{2} + C_c \frac{(\dot{\phi}_J - \sum_{m=0}^{m < M} \dot{\phi}_m)^2}{2} + \sum_{m=0}^{m < M} C_0 \frac{(\dot{\phi}_m)^2}{2} \\ & + E_J \cos\left(2\pi \frac{\phi_J}{\Phi_0}\right) - \sum_{m=0}^{m < M} (2m+1)^2 \frac{(\phi_m)^2}{2L_0}. \end{aligned} \quad (\text{S8})$$

Now the variables ϕ_m correspond directly to the voltage difference across the capacitance of the m -th LC oscillator. With the objective of writing a Hamiltonian, it is useful to express the capacitive part of the Lagrangian in matrix notation

$$\mathcal{L} = \frac{1}{2} \dot{\phi}^T \mathbf{C} \dot{\phi} + E_J \cos\left(2\pi \frac{\phi_J}{\Phi_0}\right) - \sum_{m=0}^{m < M} (2m+1)^2 \frac{(\phi_m)^2}{2L_0}, \quad (\text{S9})$$

$$\dot{\phi}^T = [\dot{\phi}_J \ \dot{\phi}_0 \ \dot{\phi}_1 \ \dot{\phi}_2 \ \cdots \ \dot{\phi}_{M-1}], \quad (\text{S10})$$

$$\mathbf{C} = \begin{bmatrix} C_J + C_c & -C_c & -C_c & -C_c & \cdots & -C_c \\ -C_c & C_0 + C_c & C_c & C_c & \cdots & C_c \\ -C_c & C_c & C_0 + C_c & C_c & & \\ -C_c & C_c & C_c & C_0 + C_c & & \\ \vdots & \vdots & & & \ddots & \\ -C_c & C_c & & & & C_0 + C_c \end{bmatrix}. \quad (\text{S11})$$

The canonical momenta (dimensionally charges) are equal to

$$q_i = \frac{\partial \mathcal{L}}{\partial \dot{\phi}_i} = C_{ij} \dot{\phi}_i \quad (\text{S12})$$

using Einstein summation convention for repeated indices. The Hamiltonian $H = q_i \dot{\phi}_i - \mathcal{L}$ is then given by

$$H = \frac{1}{2} \mathbf{q}^T \mathbf{C}^{-1} \mathbf{q} - E_J \cos\left(2\pi \frac{\phi_J}{\Phi_0}\right) + \sum_{m=0}^{m < M} (2m+1)^2 \frac{(\phi_m)^2}{2L_0}, \quad (\text{S13})$$

$$\mathbf{q}^T = [q_B \ q_0 \ q_1 \ q_2 \ \cdots \ q_{M-1}] \quad (\text{S14})$$

and the inverse of the capacitance matrix is

$$\mathbf{C}^{-1} = \frac{1}{C_0(MC_cC_J + C_0(C_c + C_J))} \times \begin{bmatrix} C_0^2 + MC_0C_c & C_0C_c & C_0C_c & \cdots \\ C_0C_c & C_0(C_c + C_J) + (M-1)C_cC_J & -C_JC_c & \cdots \\ C_0C_c & -C_JC_c & C_0(C_c + C_J) + (M-1)C_cC_J & \cdots \\ \vdots & \vdots & \vdots & \ddots \end{bmatrix}. \quad (\text{S15})$$

It is easy to check this result in a very general way by verifying that $\mathbf{C}\mathbf{C}^{-1} = \mathbf{C}^{-1}\mathbf{C} = \mathbf{I}$. We now quantize the canonical variables $q_i \rightarrow \hat{q}_i$, $\phi_i \rightarrow \hat{\phi}_i$, postulating the commutation relation

$$[\hat{\phi}_i, \hat{q}_j] = i\hbar\delta_{ij}. \quad (\text{S16})$$

This results in the Hamiltonian

$$\hat{H}^{(M)} = \hat{H}_{\text{AA}}^{(M)} + \hat{H}_{\text{cav}}^{(M)} + \hat{H}_{\text{int}}^{(M)}. \quad (\text{S17})$$

The AA Hamiltonian is defined as

$$\hat{H}_{\text{AA}}^{(M)} = \frac{1}{2C_{\text{AA}}^{(M)}}\hat{q}_B^2 - E_J \cos\left(2\pi\frac{\phi_J}{\Phi_0}\right), \quad (\text{S18})$$

where the atoms capacitance is given by

$$C_{\text{AA}}^{(M)} = \frac{C_0(MC_cC_J + C_0(C_c + C_J))}{C_0^2 + MC_0C_c}. \quad (\text{S19})$$

Usually, the charge is expressed in number of Cooper pairs $\hat{q}_B = 2e\hat{N}_J$ and the charging energy is given by $E_C^{(M)} = e^2/2C_{\text{AA}}^{(M)}$, resulting in the Hamiltonian

$$\hat{H}_{\text{AA}}^{(M)} = 4E_C^{(M)}\hat{N}_J^2 - E_J \cos\left(2\pi\frac{\hat{\phi}_J}{\Phi_0}\right). \quad (\text{S20})$$

In the main text, we introduced the superconducting phase difference across the junction as $\hat{\delta} = 2\pi\frac{\hat{\phi}_J}{\Phi_0}$. The cavity Hamiltonian is equal to

$$\hat{H}_{\text{cav}}^{(M)} = \sum_{m=0}^{m<M} \frac{1}{2C_0^{(M)}}\hat{q}_m^2 + \sum_{m=0}^{m<M} (2m+1)^2 \frac{(\phi_m)^2}{2L_0}, \quad (\text{S21})$$

where the effective capacitance of each oscillator is given by

$$C_0^{(M)} = \frac{C_0(MC_cC_J + C_0(C_c + C_J))}{(M-1)C_cC_J + C_0(C_c + C_J)}. \quad (\text{S22})$$

We define the creation and annihilation operators

$$\hat{\phi}_m = \frac{-i}{\sqrt{2m+1}} \sqrt{\frac{\hbar}{2} \sqrt{\frac{L_0}{C_0^{(M)}}}} (\hat{a}_m - \hat{a}_m^\dagger), \quad (\text{S23})$$

$$\hat{q}_m = \sqrt{2m+1} \sqrt{\frac{\hbar}{2} \sqrt{\frac{C_0^{(M)}}{L_0}}} (\hat{a}_m + \hat{a}_m^\dagger), \quad (\text{S24})$$

reducing the cavity Hamiltonian to

$$\hat{H}_{\text{cav}}^{(M)} = \sum_{m=0}^{m<M} \hbar\omega_m^{(M)} \hat{a}^\dagger \hat{a}, \quad (\text{S25})$$

$$\omega_m^{(M)} = \frac{2m+1}{\sqrt{L_0 C_0^{(M)}}}, \quad (\text{S26})$$

where we have dropped the constant energy contributions $\hbar\omega_m^{(M)}/2$. The quantum voltage of each mode is

$$\hat{V}_m^{(M)} = \frac{\hat{Q}_m}{C_0^{(M)}} = V_{\text{zpf},m}^{(M)} (\hat{a}_m + \hat{a}_m^\dagger), \quad (\text{S27})$$

defining the zero point fluctuations of the m -th mode by $V_{\text{zpf},m}^{(M)} = \sqrt{2m+1} \sqrt{\hbar\omega_0^{(M)}/2C_0^{(M)}}$.

The interaction term $\hat{H}_{\text{int}}^{(M)}$ is given by

$$\hat{H}_{\text{int}}^{(M)} = \sum_{m=0}^{m < M} \sum_{m'=m+1}^{m' < M} G_{m,m'}^{(M)} (a_m + a_m^\dagger)(a_{m'} + a_{m'}^\dagger) + \sum_{m=0}^{m < M} \hbar\bar{g}_m^{(M)} \hat{N}_J (a_m + a_m^\dagger), \quad (\text{S28})$$

where $G_{m,m'}^{(M)}$ quantifies the coupling between the m -th and m' -th modes of the resonator through the presence of the capacitances introduced by the AA

$$G_{m,m'}^{(M)} = -\frac{C_0 C_c C_J}{M C_c C_J + C_0 (C_c + C_J)} \frac{(C_0^{(M)})^2}{C_0^2} V_{\text{zpf},m}^{(M)} V_{\text{zpf},m'}^{(M)}, \quad (\text{S29})$$

and $\hbar\bar{g}_m^{(M)} = \beta^{(M)} V_{\text{zpf},m}^{(M)} 2e$ quantifies the coupling between the m -th mode of the resonator and the AA. It is weighted by the capacitance ratio

$$\beta^{(M)} = \frac{C_0 C_c}{M C_c C_J + C_0 (C_c + C_J)} \frac{C_0^{(M)}}{C_0}. \quad (\text{S30})$$

We can also write the Hamiltonian in the basis of eigenstates of the AA Hamiltonian. Defining the eigenstates $\{|i\rangle^{(M)}\}$ and eigenvalues $\epsilon_i^{(M)}$ by $\hat{H}_{\text{AA}}^{(M)} |i\rangle^{(M)} = \hbar\epsilon_i^{(M)} |i\rangle^{(M)}$ and making the transformation $\hat{H}^{(M)} \rightarrow \sum_i |i\rangle^{(M)} \langle i|^{(M)} \hat{H}^{(M)} \sum_j |j\rangle^{(M)} \langle j|^{(M)}$ we obtain the final form of the Hamiltonian

$$\begin{aligned} \hat{H}^{(M)} &= \sum_{m=0}^{m < M} \hbar\omega_m^{(M)} \hat{a}_m^\dagger \hat{a}_m \\ &+ \sum_i \hbar\epsilon_i^{(M)} |i\rangle^{(M)} \langle i|^{(M)} \\ &+ \sum_{i,j} \sum_{m=0}^{m < M} \hbar g_{m,i,j}^{(M)} |i\rangle^{(M)} \langle j|^{(M)} (\hat{a}_m + \hat{a}_m^\dagger) \\ &+ \sum_{m=0}^{m < M} \sum_{m'=m+1}^{m' < M} G_{m,m'}^{(M)} (\hat{a}_m + \hat{a}_m^\dagger)(a_{m'} + a_{m'}^\dagger) \end{aligned} \quad (\text{S31})$$

where the coupling $g_{m,i,j}$ is given by:

$$\hbar g_{m,i,j} = V_{\text{zpf},m}^{(M)} 2e\beta^{(M)} \langle i|^{(M)} \hat{N}_J |j\rangle^{(M)}. \quad (\text{S32})$$

If $C_J = 0$, this Hamiltonian reduces to the one given in the main text. If not we can make use of a Bogoliubov transformation to express it in terms of the eigenmodes of the resonator as described in the Sec. S4. This would allow us to recover the form of the Hamiltonian given in the main text. Alternatively the above hamiltonian can be diagonalized as it is to obtain an energy spectrum.

S2. DISPERSIVE SHIFT OF COUPLED LC OSCILLATORS

In this section, we derive the Lamb shift of a linearized AA (i.e. a series LC oscillator) dispersively coupled to a single resonator mode for the case $C_J = 0$ as shown in Fig. S2. The atom is linearized by discarding the purely

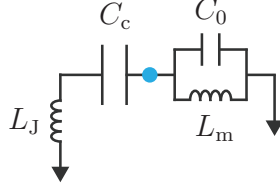


FIG. S2. Circuit of a linearized AA (series LC oscillator) coupled to a single mode m of the resonator. Studying this circuit provides a good approximation of the Lamb shift in the Transmon regime $E_J \gg E_C$. The coupling point is shown as a blue dot.

non-linear part of the Josephson junction, leaving an inductor $L_J = \hbar^2/4e^2E_J$ [S4]. We find that this shift gives a good approximation of the Lamb shift of high modes in the Transmon regime $E_J \gg E_C^{(0)}$. We denote by L_J the inductance of the linearized AA and by L_m and C_0 the inductance and capacitance of a coupled parallel LC oscillator representing a bare resonator mode. The dispersive approximation assumes

$$\omega_m \gg \omega_a, \quad (\text{S33})$$

where ω_a is the resonance frequency of the bare linearized atom $\omega_a = 1/\sqrt{L_J C_c}$ and ω_m is the resonance frequency of the bare mode resonator $\omega_m = 1/\sqrt{L_m C}$. This condition is assumed to be met due to a small mode inductance

$$L_J \gg L_m \quad (\text{S34})$$

as is the case for high frequency modes $m \gg 1$. Resonance is reached when the input impedance of the parallel LC oscillator is equal to minus that of the series LC oscillator, which is equivalent to a boundary condition of matching voltage and current at the coupling point shown in Fig. S2. This condition reads

$$\frac{1}{iC_c\omega} + iL_J\omega = -\frac{1}{iC_0\omega + \frac{1}{iL_m\omega}}. \quad (\text{S35})$$

Introducing the bare resonance frequencies corresponding to both resonators shunted to ground at the coupling point, this equation can be rewritten

$$\omega^4 - \omega^2 \left(\omega_m^2 + \omega_a^2 + \frac{L_m}{L_J} \omega_m^2 \right) + \omega_m^2 \omega_a^2 = 0. \quad (\text{S36})$$

This equation has two positive solutions

$$\omega_{\pm} = \frac{\omega_m}{\sqrt{2}} \sqrt{1 + \frac{L_m}{L_J} + \eta \pm \sqrt{\left(1 + \frac{L_m}{L_J} + \eta\right)^2 - 4\eta}}, \quad (\text{S37})$$

where we introduced the quantity $\eta = (\omega_a/\omega_m)^2$. In the assumption of Eq. (S33), the lower resonance frequency ω_- is given to first order in η by

$$\omega_- \simeq \frac{\omega_a}{\sqrt{1 + \frac{L_m}{L_J}}}. \quad (\text{S38})$$

Introducing the second assumption given by Eq. (S34), we obtain to first order in L_m/L_J the resonance frequency

$$\omega_- \simeq \omega_a - \frac{\omega_a L_m}{2 L_J}, \quad (\text{S39})$$

which yields the value of the ‘‘classical Lamb shift’’ $\bar{\chi}_m/\hbar = -\frac{\omega_a L_m}{2 L_J}$. If we introduce the Josephson energy through $L_J = \hbar^2/4e^2E_J$, the atomic frequency $\hbar\omega_a = \sqrt{8E_J E_C^{(0)}}$ and the coupling $\hbar\gamma_m = 2e\sqrt{\frac{\hbar\omega_m}{2C_0}} \left(\frac{E_J}{32E_C^{(0)}} \right)^{\frac{1}{4}}$, this shift can be written in the language of the Rabi Hamiltonian following

$$\bar{\chi}_m/\hbar = -2 \frac{(\omega_a)^2 (\gamma_m)^2}{\omega_m^3}. \quad (\text{S40})$$

Extrapolating this formula for the case of a non-linearized atom in the Transmon regime by making the approximations $\omega_a^{(0)} \simeq \omega_a$ and $g_m^{(0)} \simeq \gamma_m$ we obtain the formula for the Lamb shift presented in the main text

$$\chi_m/\hbar \simeq -2 \frac{(\omega_a^{(0)})^2 (g_m^{(0)})^2}{\omega_m^3} . \quad (\text{S41})$$

S3. NUMERICAL METHODS

In order to perform numerical calculations, we first diagonalize the AA Hamiltonian $\hat{H}_{\text{AA}}^{(M)}$ (also known as Cooper pair box Hamiltonian) in the charge basis $\{|N_J\rangle\}_{N_J=-N_{\text{max}}, \dots, +N_{\text{max}}}$ where $|N_J\rangle$ is an eigenstate of \hat{N}_J . In this basis the Josephson junction term is given by (see Ref. [S5])

$$\cos(\hat{\delta}) = \frac{1}{2} \sum_{N=-\infty}^{+\infty} |N_J\rangle \langle N_J + 1| + |N_J + 1\rangle \langle N_J| . \quad (\text{S42})$$

The basis is truncated to a certain number of Cooper pairs $\pm N_{\text{max}}$. We found that using more than $N_{\text{max}} = 20$ has little impact on simulation results for our set of example parameters. After diagonalization of H_{AA} we can inject the values for $\epsilon_i^{(M)}$ and $\langle i | \hat{N}_J | j \rangle^{(M)}$ into the Hamiltonian $\hat{H}^{(M)}$ which we in turn diagonalize. Numerical calculations are performed using the Python library QuTIP [S6].

What must ensue is a careful choice of the size of the Hilbert space, namely the number of photon levels n_m for the mode m as well as the number of AA levels n_a . Note that the size of the Hilbert space scales as $2^{n_a} \prod_{m=0}^{M-1} n_m$. We find that a high number of photon levels are needed for convergence. This is particularly true for the modes which are the closest (in frequency) to $\omega_{ge}^{(0)}$. This is illustrated in Fig. S3 and explains the difficulty of providing a good estimate for the effective Lamb shift through a simple application of perturbation theory.

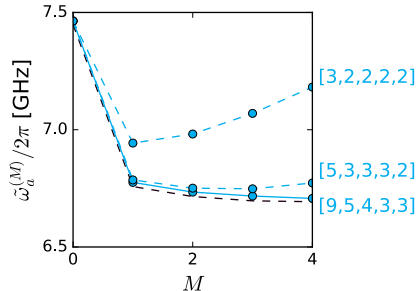


FIG. S3. The blue dots correspond to calculations of the dressed first AA transition frequency as we increase the number of modes included in the circuit model. Associated to each line is an array of integers, the first number of the array corresponds to the number of AA levels included in the model, and the following numbers correspond to the number of photon levels included, ordered with increasing mode frequency. Including less photon levels in the modes and in the AA leads to divergences. The dashed black line is the result of applying black box quantization to the M mode lumped element equivalent circuit of the system.

S4. BOGOLIUBOV TRANSFORMATION

In the case $C_J \neq 0$, one way to recover the form of the Hamiltonian presented in the main text is through a Bogoliubov transformation as described in this section. In the Hamiltonian given by Eq. (S31), the energy of the bare resonator modes and the mode-mode coupling term correspond to the Hamiltonian of M coupled harmonic oscillators

$$\hat{H}' = \sum_{m=0}^{m < M} \hbar \omega_m^{(M)} \hat{a}_m^\dagger \hat{a}_m + \sum_{m=0}^{m < M} \sum_{m'=m+1}^{m < M} G_{m,m'}^{(M)} (\hat{a}_m + \hat{a}_m^\dagger) (a_{m'} + a_{m'}^\dagger) , \quad (\text{S43})$$

which can be diagonalized through a Bogoliubov transformation even for M on the order of thousands [S7]. We start by writing Eq. (S43) as follows

$$\hat{H}' = \sum_{m,m'=0}^{m,m'<M} [\eta_{m,m'}(\hat{a}_m a_{m'} + \hat{a}_m^\dagger a_{m'}^\dagger) + \xi_{m,m'}(\hat{a}_m^\dagger a_{m'} + \hat{a}_m a_{m'}^\dagger)] , \quad (\text{S44})$$

or, in matrix notation

$$\hat{H}' = \boldsymbol{\alpha}^T \mathbf{h}' \boldsymbol{\alpha} , \quad (\text{S45})$$

where $\boldsymbol{\alpha}$ is a vector of the annihilation and creation operators

$$\boldsymbol{\alpha}^T = [\hat{a}_0, \hat{a}_1, \dots, \hat{a}_{M-1}, \hat{a}_0^\dagger, \hat{a}_1^\dagger, \dots, \hat{a}_{M-1}^\dagger] , \quad (\text{S46})$$

and \mathbf{h}' is the matrix

$$\mathbf{h}' = \begin{bmatrix} \boldsymbol{\eta} & \boldsymbol{\xi} \\ \boldsymbol{\xi} & \boldsymbol{\eta} \end{bmatrix} . \quad (\text{S47})$$

In this case $\eta_{m,m'} = \xi_{m,m'} = G_{m,m'}^{(M)}/2$ if $m \neq m'$ and $\eta_{m,m} = 0$, $\xi_{m,m} = \hbar\omega_m^{(M)}/2$ otherwise. The challenge is now to find a matrix that maps $\boldsymbol{\alpha}$ to a new set of creation and annihilation operators $\boldsymbol{\beta}$,

$$\boldsymbol{\beta}^T = [\hat{b}_0, \hat{b}_1, \dots, \hat{b}_{M-1}, \hat{b}_0^\dagger, \hat{b}_1^\dagger, \dots, \hat{b}_{M-1}^\dagger] , \quad (\text{S48})$$

which diagonalize \hat{H}' whilst maintaining the expected commutation relations $[\hat{b}_m, \hat{b}_{m'}^\dagger] = \delta_{m,m'}$. Following the method described in Ref. [S7], we introduce the matrix

$$\mathbf{J} = \begin{bmatrix} \mathbf{0} & \mathbf{I} \\ -\mathbf{I} & \mathbf{0} \end{bmatrix} , \quad (\text{S49})$$

where \mathbf{I} ($\mathbf{0}$) is an $M \times M$ identity (zero) matrix. Diagonalizing the matrix $\mathbf{h}'\mathbf{J}$ yields eigenvalues that come in pairs such that if μ is an eigenvalue, then $-\mu$ is too. We order the eigenvalues and eigenstates such that the negative eigenvalues come first, in order of increasing absolute value, and the corresponding positive eigenvalues next, in the same order. We use the following notation for these eigenvalues

$$[-\mu_0, -\mu_1, \dots, -\mu_{M-1}, \mu_0, \mu_1, \dots, \mu_{M-1}] . \quad (\text{S50})$$

We then construct a matrix \mathbf{F} with the eigenvectors as columns and normalize them such that the \mathbf{F} is symplectic: $\mathbf{F}^T \mathbf{J} \mathbf{F} = \mathbf{J}$. To do so, we normalize each eigenvector v_m such that $\sum_{i=0}^{i<2M} (v_m)_i^2 = 1$ and flip the sign of certain eigenvectors such that the first coefficient of v_m (with eigenvalue $-\mu_m$) has the same sign as the M -th coefficient of v_{m+M} (with eigenvalue μ_m). The matrix thus constructed should be of the form

$$\mathbf{F} = \begin{bmatrix} \mathbf{A} & \mathbf{B} \\ \mathbf{B} & \mathbf{A} \end{bmatrix} . \quad (\text{S51})$$

By defining the vector of annihilation and creation operators $\boldsymbol{\beta}$ as $\boldsymbol{\alpha} = \mathbf{A}\boldsymbol{\beta} - \mathbf{B}\boldsymbol{\beta}^\dagger$, we have defined a basis which diagonalizes \hat{H}'

$$\hat{H}' = \sum_{m=0}^{m<M} 2\mu_m^{(M)} \hat{b}_m^\dagger \hat{b}_m , \quad (\text{S52})$$

the new eigenenergies in fact being given by the eigenvalues of the previously diagonalized matrix. In this basis, the atom-mode interaction term becomes

$$\hat{H}_{\text{int}}^{(M)} = \sum_{i,j} \sum_{m=0}^{m<M} \left[\sum_{m'=0}^{m'<M} \hbar g_{m',i,j}^{(M)} (\mathbf{A} - \mathbf{B})_{m',m} \right] |i\rangle^{(M)} \langle j|^{(M)} (\hat{b}_m + \hat{b}_m^\dagger) , \quad (\text{S53})$$

and we recover the extended Rabi Hamiltonian structure by defining the coupling as

$$g_{m,i,j}^{(M)} = \sum_{m'=0}^{m'<M} \hbar g_{m',i,j}^{(M)} (\mathbf{A} - \mathbf{B})_{m',m} . \quad (\text{S54})$$

This coupling strength was plotted in the main text. In Fig. S4, we plot the frequencies of the newly defined eigenmodes of the resonator. As expected, these transition from the eigenfrequencies of a $\lambda/4$ resonator to those of a $\lambda/2$. In Fig. S5, we show the same plot as in Fig. 3 of the main text but for $C_J = 5$ fF, the result of diagonalizing the Hamiltonian derived above.

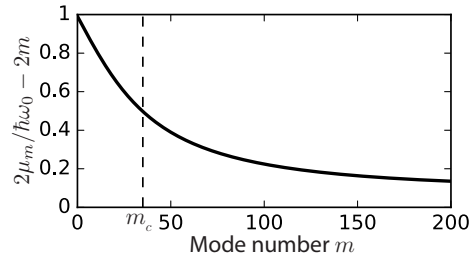


FIG. S4. Mode frequency as a function of the number of modes in the case $C_J = 5$ fF (other circuit parameters fixed in the main text). The critical mode m_C marks a transition from the regime where the resonator acts as a $\lambda/4$ resonator, with frequencies $2\mu_m \simeq (2m + 1)\omega_0$ to a regime where the resonator becomes a $\lambda/2$ resonator, with eigenfrequencies $2\mu_m \rightarrow 2m\omega_0$.

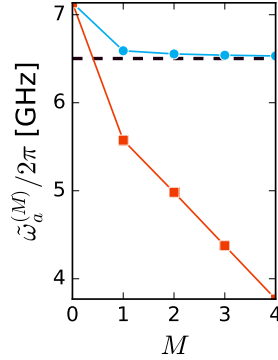


FIG. S5. Convergence of the spectrum in the case $C_J = 5$ fF (other circuit parameters fixed in the main text). We plot the $|g\rangle \rightarrow |e\rangle$ transition frequency of the atom dispersively shifted by M resonator modes as a function of M . Dots (squares) correspond to an exact diagonalization of the circuit (non-)renormalized multi-mode Rabi model. The frequency obtained by Black-box quantization (dashed line) provides a point of reference corresponding to the case when all modes are included.

S5. DRESSING OF THE ATOMIC CHARGING ENERGY

The Hamiltonian $H^{(M+1)}$ with $M + 1$ bosonic modes coupled to the Josephson junction (Eq. (1) of the Letter) lives in the Hilbert space $\mathcal{H}^{(M+1)} = \mathcal{H}_{N_J} \otimes_{m \leq M} \mathcal{H}_m$

$$H^{(M+1)} = \hbar\omega_M a_M^\dagger a_M + \hbar\bar{g}_M (a_M + a_M^\dagger) \hat{N}_J + H^{(M)} \quad (\text{S55})$$

$$= \hbar\omega_M \left(a_M^\dagger + \frac{\bar{g}_M}{\omega_M} \hat{N}_J \right) \left(a_M + \frac{\bar{g}_M}{\omega_M} \hat{N}_J \right) + H^{(M)} - \hbar \frac{\bar{g}_M^2}{\omega_M} \hat{N}_J^2 \quad (\text{S56})$$

$$= \hbar\omega_M b_M^\dagger b_M + \tilde{H}^{(M)}, \quad (\text{S57})$$

where we have defined the bosonic operators

$$b_M = a_M + \frac{\bar{g}_M}{\omega_M} \hat{N}_J, \quad (\text{S58})$$

$$b_M^\dagger = a_M^\dagger + \frac{\bar{g}_M}{\omega_M} \hat{N}_J, \quad (\text{S59})$$

and the Hamiltonian

$$\tilde{H}^{(M)} = H^{(M)} - \hbar \frac{\bar{g}_M^2}{\omega_M} \hat{N}_J^2 \quad (\text{S60})$$

We look for an effective Hamiltonian which approximates the low energy part of $H^{(M+1)}$. The pair b_M, b_M^\dagger are canonically conjugate, $[b_M, b_M^\dagger] = 1$. Thus, $b_M^\dagger b_M$ is a number operator. If $\hbar\omega_M$ is much larger than the characteristic energy of the low energy sector of $\tilde{H}^{(M)}$, the low energy sector of $H^{(M+1)}$ will be well approximated by setting $b_M^\dagger b_M$ to zero. That is, by studying the restriction of $H^{(M+1)}$ to the vacuum subspace of b_M , namely

$$\mathcal{S}^{(M+1)} = \{|\Psi\rangle / b_M |\Psi\rangle = 0\}. \quad (\text{S61})$$

In order that the separation of scales that has been assumed indeed holds, it is also imperative that $\tilde{H}^{(M)}$ acting on $\mathcal{S}^{(M+1)}$ results in states neighbouring $\mathcal{S}^{(M+1)}$. That is to say, that the commutator $[b_M, \tilde{H}^{(M)}]$ acting on $\mathcal{S}^{(M+1)}$ be small. In the case at hand,

$$[b_M, \tilde{H}^{(M)}] = \frac{\bar{g}_M}{\omega_M} [\hat{N}_J, H^{(M)}] \quad (\text{S62})$$

$$= i \frac{E_J \bar{g}_M}{\omega_M} \sin(\varphi_J), \quad (\text{S63})$$

so if $E_J, \bar{g}_M \ll \omega_M$ then we can say that the commutator above is small, and that $\tilde{H}^{(M)}|_{\mathcal{S}^{(M+1)}}$ will provide a good effective Hamiltonian for $H^{(M+1)}$. Notice that these conditions are increasingly better fulfilled with growing mode number M for the model in the main text. We now construct explicitly the effective Hamiltonian $\tilde{H}^{(M)}|_{\mathcal{S}^{(M+1)}}$. The subspace $\mathcal{S}^{(M+1)}$ can be expanded in the following basis

$$|\alpha_{N_J}\rangle^{(M+1)} = |N_J\rangle |\beta\rangle^{(M)} |z_M = -\gamma_M N_J\rangle, \quad (\text{S64})$$

where vectors $|\beta\rangle^{(M)}$ form a basis of the truncated subspace $\otimes_{m < M} \mathcal{H}_m$, $|z_M\rangle$ is a coherent state for the $(M+1)$ -th mode and $\gamma_M = \bar{g}_M/\omega_M$. The original bosonic a_M and Cooper-Pair number \hat{N}_J operators act on this basis as

$$a_M |\alpha_{N_J}\rangle^{(M+1)} = -\gamma_M N_J |\alpha_{N_J}\rangle^{(M+1)}, \quad (\text{S65})$$

$$\hat{N}_J |\alpha_{N_J}\rangle^{(M+1)} = N_J |\alpha_{N_J}\rangle^{(M+1)}. \quad (\text{S66})$$

Thus, the matrix elements of $H^{(M+1)}|_{\mathcal{S}^{(M+1)}}$ are

$$\langle \alpha_{N_J} |^{(M+1)} H^{(M+1)} | \alpha_{M_J} \rangle^{(M+1)} = \langle -\gamma_M N_J | -\gamma_M M_J \rangle \langle \alpha_{N_J} |^{(M)} \tilde{H}^{(M)} | \alpha_{M_J} \rangle^{(M)} \quad (\text{S67})$$

$$= e^{-\gamma_M^2 (N_J - M_J)^2 / 2} \langle \alpha_{N_J} |^{(M)} \tilde{H}^{(M)} | \alpha_{M_J} \rangle^{(M)} \quad (\text{S68})$$

$$\approx \langle \alpha_{N_J} |^{(M)} \tilde{H}^{(M)} | \alpha_{M_J} \rangle^{(M)}, \quad (\text{S69})$$

where the last line gives us a further approximation, valid if $\gamma_M \ll 1$ and the low energy states of $\tilde{H}^{(M)}$ have small dispersion for \hat{N}_J . If these indeed hold, $\tilde{H}^{(M)}$ itself is a good effective Hamiltonian for $H^{(M+1)}$. We can iterate this procedure down to a mode L for which the above conditions still holds. For $M \rightarrow \infty$, an effective Hamiltonian with L modes is then given by

$$H = \sum_{m=0}^{m < L} \hbar \omega_m^{(L)} a_m^\dagger a_m + \hbar \bar{g}_m^{(L)} (a_m + a_m^\dagger) \hat{N}_J + 4\tilde{E}_C^{(L)} \hat{N}_J^2 - E_J \cos(\hat{\delta}), \quad (\text{S70})$$

$$\tilde{E}_C^{(L)} = \lim_{M \rightarrow \infty} E_C^{(M)} - \sum_{m \geq L}^M \hbar (\bar{g}_m^{(M)})^2 / 4\omega_m. \quad (\text{S71})$$

- [S1] D. M. Pozar, *Microwave Engineering* (John Wiley & Sons, New York, 2009).
[S2] M. H. Devoret, in *Quantum Fluctuations in Electrical Circuits (Les Houches Session LXIII)*, edited by S. Reynaud, E. Giacobino, and J. Zinn-Justin (Elsevier, New York, 1997).
[S3] S. M. Girvin, in *Circuit QED: Superconducting Qubits Coupled to Microwave Photons, Proceedings of the Les Houches Summer School* (Vol. 96, Oxford University Press, New York, NY, 2014).
[S4] S. E. Nigg, H. Paik, B. Vlastakis, G. Kirchmair, S. Shankar, L. Frunzio, M. H. Devoret, R. J. Schoelkopf, and S. M. Girvin, *Phys. Rev. Lett.* **108**, 1 (2012).
[S5] D. I. Schuster, *Circuit Quantum Electrodynamics*, Ph.D. thesis (2007).
[S6] J. R. Johansson, P. D. Nation, and F. Nori, *Computer Physics Communications* **184**, 1234 (2013).
[S7] J. Javanainen, *Phys. Rev. A* **54**, R3722 (1996).